Enhanced performance of cobalt ferrite encapsulated in graphitic shell by means of AC magnetically activated catalytic wet peroxide oxidation of 4-nitrophenol

Rui S. Ribeiro[a,b], Juan Gallo[c], Manuel Bañobre-López[c], Adrián M.T. Silva[b], Joaquim L. Faria[b], Helder T. Gomes[a,b,*]

[a] Centro de Investigação de Montanha (CIMO), Instituto Politécnico de Bragança, 5300-253 Bragança, Portugal.

[b] Laboratory of Separation and Reaction Engineering - Laboratory of Catalysis and Materials (LSRE-LCM), Faculdade de Engenharia, Universidade do Porto, Rua Dr. Roberto Frias, 4200-465 Porto, Portugal.

[c] Advanced (magnetic) Theranostic Nanostructures Lab. INL - International Iberian Nanotechnology Laboratory, Av. Mestre José Veiga, 4715-330 Braga, Portugal.

*Corresponding author. Tel.: +351 273 303 110; Fax: +351 273 313 051.

E-mail address: htgomes@ipb.pt

Abstract

Here we report preliminary catalytic wet peroxide oxidation (CWPO) experiments performed in the presence of an alternating current (AC) magnetic field. One ferromagnetic graphitic nanocomposite – composed by a cobalt ferrite core and a graphitic shell ($CoFe_2O_4$/MGNC), was employed in the process, here named magnetically activated catalytic wet peroxide oxidation (MA-CWPO). An aqueous solution containing 5.0 g L^{-1} of 4-nitrophenol (4-NP) to simulate a high strength polluted stream was used as model system. The experiments were performed at room temperature and atmospheric pressure, with stoichiometric amount of hydrogen peroxide (H_2O_2), pH = 3 and $CoFe_2O_4$/MGNC catalyst load = 5.0 g L^{-1} (corresponding to a 4-NP/$CoFe_2O_4$ mass ratio of 6.9, as $CoFe_2O_4$ accounts for 14.4 wt.% of $CoFe_2O_4$/MGNC). It was shown that the performance of CWPO is enhanced upon application of an AC magnetic field (frequency of 533.9 kHz and magnitude of 240 G). As a result, high 4-NP mineralization was obtained by MA-CWPO (as reflected by a total organic carbon abatement of 79% after 4 h of reaction, instead of 39% in the absence of a magnetic field). This positive effect was ascribed to the localised increase of $CoFe_2O_4$/MGNC surface temperature resulting from heat release upon exposure of the nanoparticulated catalyst to an AC magnetic field, which accelerates the catalytic decomposition of H_2O_2 via hydroxyl radicals (HO•) formation.

1. Introduction

In recent years, magnetic materials have been extensively applied in catalytic wet peroxide oxidation (CWPO), either directly as catalysts or included in different support/hybrid materials (e.g., alumina, silica, carbon materials, zeolites, pillared clays and minerals) [1-9]. The catalytic activity of these materials is mainly a consequence of the well-known ability of some metal species to promote the decomposition of hydrogen peroxide (H_2O_2) via hydroxyl radicals ($HO^{\bullet}$) formation. This reaction can be generally described by Eq. 1 [2, 8], in which M represents a metal with at least two possible oxidation states (e.g., M^{n+} and $M^{(n+1)+}$). Once formed, $HO^{\bullet}$ radicals are the effective species for the degradation of most of the organic pollutants present in waste waters [9, 10].

$$H_2O_2 + M^{n+} \rightleftarrows HO^{\bullet} + M^{(n+1)+} + OH^- \qquad (1)$$
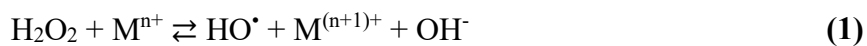
Despite all the research conducted on the application of magnetic materials in CWPO, the magnetic properties of these materials, such as their ability to locally convert magnetic induction into heat, remain unexplored [1-9]. At most, magnetic separation systems have been employed for catalyst recovery after the treatment stage. This is the case of our previous work, in which the high catalytic activity and stability of a magnetic graphitic nanocomposite (MGNC) – composed by a cobalt ferrite core and a graphitic shell ($CoFe_2O_4$/MGNC), was maintained through a series of five CWPO reaction/magnetic separation sequential experiments in the same vessel, with consecutive catalyst reuse [11].

On the other hand, iron-based magnetic nanomaterials, such as magnetite and cobalt ferrite, have received a great deal of attention from the biomedical research community, especially in the field of magnetic hyperthermia for cancer treatment [12-15]. This innovative treatment technique relies on the ability of magnetic nanoparticles to release heat upon exposure to an alternating current (AC) magnetic field, as a result of several heat dissipation mechanisms, including hysteresis losses, and Brownian and Néel relaxation [14-17] – a concept that can be extended to water treatment.

Seeking to further explore the potential arising from the application of magnetic materials in CWPO, by taking advantage of the heat dissipation properties of cobalt ferrite nanomaterials when exposed to an AC magnetic field, preliminary experiments were performed with the ferromagnetic $CoFe_2O_4$/MGNC catalyst developed in our previous work [11]. The coupling of the AC magnetic field to the CWPO process was here denoted as magnetically activated catalytic wet peroxide oxidation (MA-CWPO). Following the experimental methodology of our recent works, 4-nitrophenol (4-NP) was used as aqueous model system (5.0 g L^{-1}) of refractory organic pollutants typically not removed by conventional biological treatment technologies [11, 18].

2. Materials and methods

2.1. Chemicals

4-Nitrophenol (98 wt.%) and hydrogen peroxide (30% w/v) were purchased from Acros Organics and Fluka, respectively. Iron (III) chloride hexahydrate (97 wt.%), phenol (99.5 wt.%) and formaldehyde solution (37 wt.%, stabilized with methanol) were obtained from Panreac. Titanium (IV) oxysulphate (15 wt.% in diluted sulphuric acid, 99.99%), iron (II) chloride tetrahydrate (99 wt.%), copolymer pluronic F127 and sodium sulphite (98 wt.%) were purchased from Sigma-Aldrich. Sodium hydroxide (98.7 wt.%), sulphuric acid (95 wt.%), methanol (HPLC grade), glacial acetic acid (analytical reagent grade), *tert*-butanol (99.8 wt.%) and acetonitrile (HPLC grade) were obtained from Fisher Chemical. Distilled water was used throughout the work.

2.2. Catalyst preparation

$CoFe_2O_4$ nanoparticles were prepared by co-precipitation of Co^{2+} and Fe^{3+} in basic solution at 348.2 K, followed by thermal treatment under a purified air flow at 773.2 K. $CoFe_2O_4$/MGNC was prepared by hierarchical co-assembly of $CoFe_2O_4$ nanoparticles and carbon precursors,

followed by thermal annealing, as depicted in Figure 1. A thorough description of the synthesis procedure can be found in our previous publication [11].

FIGURE 1

2.3. Magnetic properties characterization

The magnetic properties of $CoFe_2O_4/MGNC$ were characterized with a superconducting quantum interference vibrating sample magnetometer (SQUID-VSM) from Quantum Design, adapting the procedure described elsewhere [19]. For that purpose, the hysteresis curves were obtained for magnetic fields in the range -20 – 20 kOe, at 300 K. The temperature-dependent magnetization was obtained under zero-field-cooling and field-cooling (ZFC-FC) conditions for temperatures in the range 2 – 300 K, with an applied magnetic field of 100 Oe. The magnetic properties of the catalyst recovered after a MA-CWPO run were also characterized. In this case, the catalyst was recovered after the reaction stage, washed and dried overnight in an oven at 60 ºC. Afterwards, its magnetic properties were characterized according to the above described experimental procedures.

2.4. Magnetically activated experiments

Batch CWPO experiments in the presence and absence of an AC magnetic field were performed at room temperature (297.2 ± 0.4 K), in a 100 mL glass beaker with mechanical stirring (700 rpm). The beaker was loaded with 4-NP aqueous solutions (5.0 g L^{-1}, i.e. 0.036 M). In magnetically activated catalytic wet peroxide oxidation (MA-CWPO) runs, the beaker was placed inside of an electromagnetic coil to allow the application of an AC magnetic field (cf. Figure 2). The pH of the 4-NP solutions was previously adjusted to 3 by means of H_2SO_4 and NaOH solutions. The experiments were allowed to proceed freely, without further pH conditioning. H_2O_2 (30% w/v) was then injected into the system, in order to reach the non-catalytic stoichiometric amount of H_2O_2 needed to completely mineralise 4-NP (17.8 g L^{-1}; i.e., considering the direct reaction of 4-NP with H_2O_2, leading to the formation of carbon dioxide,

water and nitrate). The catalyst was added after complete homogenization of the resulting solution, that moment being considered as $t_0 = 0$ min. The AC magnetic field was applied with a frequency of 533.9 kHz and a nominal coil field at maximum of 240 G. A Magnetherm[TM] apparatus (NanoTherics Ltd) equipped with a water-cooling system was used in order to control the electromagnetic coil temperature. The experimental set-up is shown in Figure 2.

A pure adsorption run was performed in order to assess the possible influence of adsorption on the 4-NP removal by CWPO, but, in this case, the amount of H_2O_2 was replaced by distilled water. A blank experiment, without any catalyst, was carried out to assess possible non-catalytic oxidation promoted by H_2O_2. A MA-CWPO run was performed in the presence of *tert*-butanol (*t*-BuOH; 0.809 M), which is a known scavenger of HO$^\bullet$ radicals [20] that allows to indirectly predict the participation of these radicals in the process. All these three experiments were performed under the same AC magnetic field conditions. Room and solution temperatures were monitored during the experiments. All the experiments were performed considering the mass ratio [4-NP]$_0$/[CoFe$_2$O$_4$] = 6.9, corresponding to a mass ratio [4-NP]$_0$/[CoFe$_2$O$_4$/MGNC] = 1 (14.4 wt.% of CoFe$_2$O$_4$ in CoFe$_2$O$_4$/MGNC, as determined by thermogravimetric analysis in our previous publication [11]). A homogeneous CWPO run was performed using iron (II) chloride tetrahydrate and cobalt (II) chloride hexahydrate as source of Fe^{2+} and Co^{2+}, respectively.

FIGURE 2

2.5. Analytical methods

The amounts of 4-NP and oxidation by-products were determined by high performance liquid chromatography (HPLC). The amount of H_2O_2 was determined by a colorimetric method. Additional details on these analytical methods can be found elsewhere [18]. Total organic carbon (TOC) was determined using a Shimadzu TOC-L CSN analyser. Dissolved iron and

cobalt contents were determined by inductively coupled plasma optical emission spectrometry (ICP-OES).

3. Results and discussion

3.1. Catalyst characterization

The $CoFe_2O_4$/MGNC material was thoroughly characterized previously [11]. Nevertheless, the most relevant features are herein briefly referred. $CoFe_2O_4$/MGNC is a core-shell hybrid material obtained by encapsulation of $CoFe_2O_4$ nanoparticles within a carbon framework (cf. Figure 1). Cobalt ferrite (a = 8.363 Å), iron (a = 2.858 Å) and graphite were identified in the X-ray diffraction (XRD) pattern of $CoFe_2O_4$/MGNC. The average size of the magnetic cores of $CoFe_2O_4$/MGNC is 56 ± 18 nm, as determined from transmission electron microscopy (TEM) measurements. $CoFe_2O_4$ accounts for 14.4 wt.% of $CoFe_2O_4$/MGNC (as determined by thermogravimetric analysis), which is a micro-mesoporous material with an average pore diameter of 3.75 nm and a specific surface area (S_{BET}) of 330 $m^2 g^{-1}$. Please refer to our previous publication for additional details [11].

Regarding the magnetic properties, the hysteresis loops (M $vs.$ H) of $CoFe_2O_4$/MGNC revealed a saturation magnetization (M_s) of 24.2 emu g^{-1}, coercivity (H_c) of 0.54 kOe, and saturation remanence (M_r) of 4.9 emu g^{-1} (cf. Figure 3a), which are characteristic of ferromagnetic materials [15]. In addition, the absence of an interception point between the zero-field-cooling (ZFC) and the field-cooling (FC) magnetization curves (cf. Figure 3b) shows that the blocking temperature (T_b) of $CoFe_2O_4$/MGNC is above 300 K, further indicating that its magnetic core size is above the single-to-multidomain limit (~ 6-7 nm) [21] and so confirming its ferromagnetic behaviour .

FIGURE 3

3.2. Magnetically activated catalytic wet peroxide oxidation

CoFe$_2$O$_4$/MGNC was employed in batch CWPO and MA-CWPO experiments performed in the absence and presence of an AC magnetic field, respectively. Additional experiments were performed in order to assess the possible contribution of adsorption and non-catalytic conversion on the 4-NP removal by CWPO and MA-CWPO. All the experiments were performed at room temperature (297.2 ± 0.4 K), using the experimental set-up depicted in Figure 2. Except for the CWPO run, in which the electric current was switched OFF, the experiments depicted in Figure 4 were performed under the influence of the AC magnetic field described in Section 2.4. As observed, the 4-NP removal obtained after 3 h of CWPO amounts to 27.7% of its initial content. This result apparently shows that the application of CoFe$_2$O$_4$/MGNC by itself enables the CWPO of 4-NP under the operating conditions employed. However, a detailed analysis reveals that the 4-NP removal obtained by CWPO matches the sum of the 4-NP removals obtained by adsorption and non-catalytic conversion promoted by H$_2$O$_2$. Specifically, the 4-NP removal obtained in the non-catalytic run (i.e., in the absence of catalyst) was 11.7%, while the 4-NP removal obtained in pure adsorption run was 16.6% of its initial content. Since both effects should occur simultaneously in the presence of the solid catalyst and they compete with the H$_2$O$_2$ assisted process in the CWPO, it is expected that the conversion of 4-NP overcomes that of H$_2$O$_2$ (given that the latter is in stoichiometric amount). In fact, in the presence of the catalyst depending on the regime of mass transfer the three processes can coexist accounting for the observed discrepancy. This cumulative effect of non-catalytic conversion and adsorption explains why 4-NP conversion is higher than H$_2$O$_2$ conversion in the CWPO run. A similar phenomenon was observed concerning TOC conversion (cf. Figure 4). Bearing this in mind, it is possible to conclude that the CWPO system is inefficient for the removal of 4-NP under the operating conditions considered. Nevertheless, a 2.2-fold increase, both in 4-NP and TOC conversions, is obtained when CWPO is performed in the presence of the AC magnetic field, through the process here named as magnetically

activated catalytic wet peroxide oxidation (MA-CWPO). Likewise, a 2.4-fold increase in H_2O_2 consumption is observed (cf. Figure 4). It should be noted that both 4-NP and TOC conversions are higher than H_2O_2 conversion in the MA-CWPO run. This phenomenon can be explained by the cumulative effect of adsorption and catalytic conversion.

The results obtained up to this point suggest that the performance of CWPO in the presence of the ferromagnetic $CoFe_2O_4$/MGNC catalyst is enhanced upon application of an AC magnetic field. Additional experiments were performed in order to provide further insights on the reaction mechanisms involved in the MA-CWPO process. Since CWPO relies on the formation of $HO^{\bullet}$ radicals through the reaction described by Eq. 1, the participation of this species in the MA-CWPO process was evaluated. For that purpose, *tert*-butanol (*t*-BuOH) – a strong $HO^{\bullet}$ radical scavenger [20, 22], was added before a MA-CWPO run performed in the presence of $CoFe_2O_4$/MGNC. As observed in Figure 4, the 4-NP removal is suppressed by *t*-BuOH. Specifically, the 4-NP removal decreases to 28.3% of its initial content, which, as previously discussed for the CWPO run, may be ascribed to adsorption and non-catalytic removal promoted by H_2O_2. Therefore, this indirect result suggests that $HO^{\bullet}$ radicals are effectively formed during MA-CWPO performed in the presence of $CoFe_2O_4$/MGNC. It should be noted that TOC was not measured in the experiment performed with *t*-BuOH (cf. Figure 4). This radical scavenger contributes itself to increasing the TOC content, which would affect the significance of the results obtained in this way.

FIGURE 4

Additional details on H_2O_2, 4-NP and TOC conversions as a function of time in the MA-CWPO run are given in Figure 5a. As observed, if the MA-CWPO reaction is allowed to proceed during 4 h, the 4-NP conversion reaches 81.3%, representing an average pollutant mass removal rate of 203.4 mg g^{-1} h^{-1}. Direct CO_2 formation was not followed in this study. Organic carbon mineralization from 4-NP (most likely to CO_2) was followed by TOC measurements. It was found that the mineralization levels are also very high (as reflected by a TOC abatement of

9

79% after 4 h of reaction, instead of 39% in the absence of the AC magnetic field), revealing the high efficiency of the MA-CWPO process operated at room temperature. The metal leaching from the $CoFe_2O_4$/MGNC catalyst was determined at the end of the MA-CWPO run depicted in Figure 5a. The iron leaching in the treated water amounts to 1.1 mg L^{-1}, a low value when compared to the limit of 2.0 mg L^{-1} allowed in Portugal and other EU countries for the discharge of treated waters into natural water bodies. The cobalt leaching amounts to 2.1 mg L^{-1}, confirming the higher susceptibility of this metal to undergo leaching to the treated waters [23]. Nevertheless, in this case, there is a lack of discharge limits for treated wastewater and even for drinking water [24].

Concerning the assessment of a possible contribution of metal leaching on 4-NP conversion, we performed a homogeneous CWPO run. For that purpose, a solution containing Fe^{2+} and Co^{2+}, with the same concentration as that determined at the end of the MA-CWPO run (i.e., 1.1 and 2.1 mg L^{-1}, respectively), was employed as catalyst in the absence of the magnetic field. This approach represents a hypothetical scenario, in which all the metals are leached immediately at the beginning of the MA-CWPO run. Nevertheless, even under these conditions the results show that the 4-NP removal obtained is negligible (cf. Figure 5a), since it is only ca. 6% higher than that obtained in the non-catalytic run (i.e., in the absence of catalyst; cf. Figure 4). These observations highlight the heterogeneous nature of the MA-CWPO process performed in the presence of $CoFe_2O_4$/MGNC.

In order to infer about possible effects of MA-CWPO on the properties of $CoFe_2O_4$/MGNC, the catalyst was recovered after the MA-CWPO reaction stage, its magnetic properties being determined by SQUID-VSM. As observed in Figure 3a, the magnetic properties of $CoFe_2O_4$/MGNC are apparently slightly affected, the saturation magnetization (M_s) increasing from 24.2 emu g^{-1}, in the as-prepared $CoFe_2O_4$/MGNC, to 26.7 emu g^{-1}, in the used catalyst (corresponding to a 10% increase). A similar behaviour was observed regarding both coercivity (H_c) and remanent magnetization (M_r). However, it should be noted that $CoFe_2O_4$ accounts for

only 14.4 wt.% of $CoFe_2O_4$/MGNC, the remaining phase being mostly graphitic carbon. This composition makes it very difficult to compare the catalyst before and after reaction. For instance, a standard deviation of 5% was obtained upon duplicate determination of the saturation magnetization (M_s) of the as-prepared $CoFe_2O_4$/MGNC catalyst. Taking all this into account, it is suggested that the magnetic properties of $CoFe_2O_4$/MGNC are not significantly affected during its application in MA-CWPO.

The benefits of carbon encapsulation were clearly established in our previous publication devoted to the synthesis and application of a hybrid magnetic graphitic nanocomposite in CWPO [25]. In that study, the composite catalyst was prepared through the same synthesis procedure herein considered, except that magnetite was encapsulated within a graphitic shell instead of $CoFe_2O_4$ [25]. Nevertheless, in order to shed some light on the role of the carbon shell when $CoFe_2O_4$/MGNC is employed in MA-CWPO, an additional experiment was performed in the presence of bare $CoFe_2O_4$. It was found that the 4-NP removal obtained in the presence of $CoFe_2O_4$ is lower than that obtained with $CoFe_2O_4$/MGNC (cf. Figure 5a), allowing to confirm that the performance of bare $CoFe_2O_4$ in MA-CWPO is enhanced when this magnetic material is encapsulated within a graphitic structure to yield $CoFe_2O_4$/MGNC. This superior performance can be ascribed to the presence of the carbon phase, which increases the adsorptive interactions between the pollutant molecules and the surface of the catalyst, thus leading to further oxidation [25]. Please refer to our previous publication for additional details [25].

The 4-NP oxidation/mineralization mechanism by MA-CWPO was also studied. It was found that both the aromatic and non-aromatic by-products detected during the MA-CWPO experiment (cf. Figures 5b and c, respectively) are consistent with the reaction mechanism proposed in our previous studies devoted to CWPO [11, 18, 25]. Briefly, the 4-NP molecule is attacked by the HO$^\bullet$ radicals up to a point in which the aromatic ring is opened, and several low molecular weight carboxylic acids are formed. As observed in Figure 5b, most of the aromatic intermediates of 4-NP oxidation are present in low amounts; even 4-nitrocatechol, the main

aromatic intermediate of 4-NP CWPO, never surpasses a concentration around 350 mg L^{-1}. This is a very low value compared to those obtained in our previous studies devoted to the CWPO of 4-NP (in the range 1400 – 1600 mg L^{-1}, for similar 4-NP conversions) [11, 23, 25], including that performed with the CoFe$_2$O$_4$/MGNC catalyst [11]. In addition, the concentration curves in Figure 5c show that most of the carboxylic acids formed by aromatic ring opening are consequently converted afterwards. These observations highlight the high mineralization efficiency obtained by MA-CWPO in the presence of CoFe$_2$O$_4$/MGNC. At the same time, nitrates can be produced by oxidation of the –NO$_2$ group from the 4-NP molecule. The NO$_3^-$ concentration curve given in Figure 5c allows to conclude that at least 32.3% of the total nitrogen initially present in the 4-NP 5 g L^{-1} solution was effectively subtracted from the main aromatic ring after 4 h of MA-CWPO. Additional details on the reaction mechanism where previously established [18].

FIGURE 5

As discussed in Section 3.1, CoFe$_2$O$_4$/MGNC is a ferromagnetic material. It is known that these materials are able to convert magnetic energy into thermal energy, when exposed to an AC magnetic field [14-16]. In ferromagnetic materials, this phenomenon occurs mainly due to hysteresis losses, i.e., the thermal energy released in each magnetization cycle depicted in Figure 3a [16]. The solution temperature during the MA-CWPO run performed in the presence of CoFe$_2$O$_4$/MGNC was not significantly higher than that recorded during the non-catalytic experiment performed in the absence of catalyst (cf. Figure 4). These results can be explained in terms of the low CoFe$_2$O$_4$ concentration employed (0.72 g L^{-1}, corresponding to 14.4 wt.% of CoFe$_2$O$_4$/MGNC) and by CoFe$_2$O$_4$/MGNC nanoparticle agglomeration, which are crucial parameters affecting heat release [14]. These parameters were not optimized in this study. Nevertheless, the localised increase of CoFe$_2$O$_4$/MGNC surface temperature upon exposure to an AC magnetic field accounts for the superior performance of MA-CWPO for the removal of 4-NP at room temperature, when compared to that obtained by CWPO. As recently proposed

for microwave-assisted catalytic wet peroxide oxidation (MW-CWPO) [26, 27], the localised increase of $CoFe_2O_4$/MGNC surface temperature, which accelerates the catalytic decomposition of H_2O_2 via $HO^{\bullet}$ radicals formation, can be held responsible for the superior performance of MA-CWPO. Figure 6 depicts the alternative routes proposed for the 4-NP removal by CWPO and MA-CWPO.

Temperature is typically regarded as a very important operating parameter in CWPO (and in the Fenton process, a particular case of CWPO), as reflected by the recent trend for the application of higher operating temperatures (up to 398.2 K) [28-30]. Therefore, the possibility investigated in the present study to promote the decomposition of H_2O_2 via $HO^{\bullet}$ radicals formation at room temperature offers an alternative route for the development of more efficient water and wastewater treatment processes.

4. Conclusions

Here is described for the first time the tandem effect of a magnetic field on catalytic wet peroxide oxidation application, in a process here coined as magnetically activated catalytic wet peroxide oxidation (MA-CWPO).

The MA-CWPO process markedly increase both 4-NP removal and organic mineralization with respect to the non-magnetic equivalent process. This superior performance was explained by the localized increase of the surface temperature of the $CoFe_2O_4$/MGNC ferromagnetic catalyst, upon conversion of magnetic energy into thermal energy. The higher surface temperature promotes the formation of highly active sites for the catalytic decomposition of H_2O_2 via $HO^{\bullet}$ radicals formation, thus increasing the subsequent 4-NP conversion.

The results reported in this study open future prospects for the development of more efficient water and wastewater treatment processes performed at room temperature and atmospheric pressure.

References

[1] M. Munoz, Z.M. de Pedro, J.A. Casas, J.J. Rodríguez, Preparation of magnetite-based catalysts and their application in heterogeneous Fenton oxidation - A review, Appl. Catal. B 176-177 (2015) 249-265.

[2] R.S. Ribeiro, A.M.T. Silva, J.L. Figueiredo, J.L. Faria, H.T. Gomes, Catalytic wet peroxide oxidation: a route towards the application of hybrid magnetic carbon nanocomposites for the degradation of organic pollutants. A review, Appl. Catal. B 187 (2016) 428-460.

[3] P.V. Nidheesh, Heterogeneous Fenton catalysts for the abatement of organic pollutants from aqueous solution: a review, RSC Adv. 5 (2015) 40552-40577.

[4] M. Muruganandham, R.P.S. Suri, M. Sillanpää, J.J. Wu, B. Ahmmad, S. Balachandran, M. Swaminathan, Recent developments in heterogeneous catalyzed environmental remediation processes, J. Nanosci. Nanotechnol. 14 (2014) 1898-1910.

[5] S. Rahim Pouran, A.A. Abdul Raman, W.M.A. Wan Daud, Review on the application of modified iron oxides as heterogeneous catalysts in Fenton reactions, J. Cleaner Prod. 64 (2014) 24-35.

[6] M.C. Pereira, L.C.A. Oliveira, E. Murad, Iron oxide catalysts: Fenton and Fenton-like reactions - A review, Clay Miner. 47 (2012) 285-302.

[7] A. Dhakshinamoorthy, S. Navalon, M. Alvaro, H. Garcia, Metal nanoparticles as heterogeneous Fenton catalysts, ChemSusChem 5 (2012) 46-64.

[8] S. Navalon, A. Dhakshinamoorthy, M. Alvaro, H. Garcia, Heterogeneous Fenton catalysts based on activated carbon and related materials, ChemSusChem 4 (2011) 1712-1730.

[9] S. Navalon, M. Alvaro, H. Garcia, Heterogeneous Fenton catalysts based on clays, silicas and zeolites, Appl. Catal. B 99 (2010) 1-26.

[10] P.R. Gogate, A.B. Pandit, A review of imperative technologies for wastewater treatment I: oxidation technologies at ambient conditions, Adv. Environ. Res. 8 (2004) 501-551.

[11] R.S. Ribeiro, R.O. Rodrigues, A.M.T. Silva, P.B. Tavares, A.M.C. Carvalho, J.L. Figueiredo, J.L. Faria, H.T. Gomes, Hybrid magnetic graphitic nanocomposites towards catalytic wet peroxide oxidation of the liquid effluent from a mechanical biological treatment plant for municipal solid waste, Appl. Catal. B 219 (2017) 645-657.

[12] Y.V. Kolen'ko, M. Bañobre-López, C. Rodríguez-Abreu, E. Carbó-Argibay, A. Sailsman, Y. Piñeiro-Redondo, M.F. Cerqueira, D.Y. Petrovykh, K. Kovnir, O.I. Lebedev, J. Rivas, Large-scale synthesis of colloidal Fe_3O_4 nanoparticles exhibiting high heating efficiency in magnetic hyperthermia, J. Phys. Chem. C 118 (2014) 8691-8701.

[13] M. Bañobre-López, A. Teijeiro, J. Rivas, Magnetic nanoparticle-based hyperthermia for cancer treatment, Rep. Pract. Oncol. Radiother. 18 (2013) 397-400.

[14] A.E. Deatsch, B.A. Evans, Heating efficiency in magnetic nanoparticle hyperthermia, J. Magn. Magn. Mater. 354 (2014) 163-172.

[15] I. Sharifi, H. Shokrollahi, S. Amiri, Ferrite-based magnetic nanofluids used in hyperthermia applications, J. Magn. Magn. Mater. 324 (2012) 903-915.

[16] A. Hervault, N.T.K. Thanh, Magnetic nanoparticle-based therapeutic agents for thermo-chemotherapy treatment of cancer, Nanoscale 6 (2014) 11553-11573.

[17] V.F. Cardoso, A. Francesko, C. Ribeiro, M. Bañobre-López, P. Martins, S. Lanceros-Mendez, Advances in magnetic nanoparticles for biomedical applications, Adv. Healthcare Mater. 7 (2018) 1700845.

[18] R.S. Ribeiro, A.M.T. Silva, L.M. Pastrana-Martínez, J.L. Figueiredo, J.L. Faria, H.T. Gomes, Graphene-based materials for the catalytic wet peroxide oxidation of highly concentrated 4-nitrophenol solutions, Catal. Today 249 (2015) 204–212.

[19] R.O. Rodrigues, M. Bañobre-López, J. Gallo, P.B. Tavares, A.M.T. Silva, R. Lima, H.T. Gomes, Haemocompatibility of iron oxide nanoparticles synthesized for theranostic applications: a high-sensitivity microfluidic tool, J. Nanopart. Res. 18 (2016) 194.

[20] A. Aguinaco, J.P. Pocostales, J.F. García-Araya, F.J. Beltrán, Decomposition of hydrogen peroxide in the presence of activated carbons with different characteristics, J. Chem. Technol. Biotechnol. 86 (2011) 595-600.

[21] S. Gyergyek, M. Drofenik, D. Makovec, Oleic-acid-coated $CoFe_2O_4$ nanoparticles synthesized by co-precipitation and hydrothermal synthesis, Mater. Chem. Phys. 133 (2012) 515-522.

[22] W.H. Glaze, J.-W. Kang, D.H. Chapin, The chemistry of water treatment processes involving ozone, hydrogen peroxide and ultraviolet radiation, Ozone Sci. Eng. 9 (1987) 335-352.

[23] R.S. Ribeiro, A.M.T. Silva, J.L. Figueiredo, J.L. Faria, H.T. Gomes, The role of cobalt in bimetallic iron-cobalt magnetic carbon xerogels developed for catalytic wet peroxide oxidation, Catal. Today 296 (2017) 66-75.

[24] E.P. Agency, Parameters of water quality: interpretation and standards, Environmental Protection Agency, Ireland, Wexford, Ireland, 2001.

[25] R.S. Ribeiro, A.M.T. Silva, P.B. Tavares, J.L. Figueiredo, J.L. Faria, H.T. Gomes, Hybrid magnetic graphitic nanocomposites for catalytic wet peroxide oxidation applications, Catal. Today 280 (2017) 184-191.

[26] A.L. Garcia-Costa, J.A. Zazo, J.J. Rodríguez, J.A. Casas, Microwave-assisted catalytic wet peroxide oxidation. Comparison of Fe catalysts supported on activated carbon and γ-alumina, Appl. Catal. B 218 (2017) 637-642.

[27] B. Zhang, H. You, F. Wang, Microwave-enhanced catalytic wet peroxide oxidation of quinoline: the influence of pH and H_2O_2 dosage and identification of reactive oxygen species, RSC Adv. 7 (2017) 14769-14775.

[28] C.M. Domínguez, A. Quintanilla, J.A. Casas, J.J. Rodríguez, Treatment of real winery wastewater by wet oxidation at mild temperature, Sep. Purif. Technol. 129 (2014) 121-128.

[29] Y. Yan, S. Jiang, H. Zhang, Efficient catalytic wet peroxide oxidation of phenol over Fe-ZSM-5 catalyst in a fixed bed reactor, Sep. Purif. Technol. 133 (2014) 365-374.

[30] G. Pliego, J.A. Zazo, P. Garcia-Muñoz, M. Munoz, J.A. Casas, J.J. Rodríguez, Trends in the intensification of the Fenton process for wastewater treatment: an overview, Crit. Rev. Environ. Sci. Technol. 45 (2015) 2611-2692.

FIGURE CAPTIONS

Figure 1. Synthesis of $CoFe_2O_4$/MGNC by hierarchical co-assembly of $CoFe_2O_4$ nanoparticles and carbon precursors, followed by thermal treatment.

Figure 2. Experimental set-up used for the MA-CWPO experiments: (a) front view and (b) schematic representation. Inset of (a): top view of the coil region.
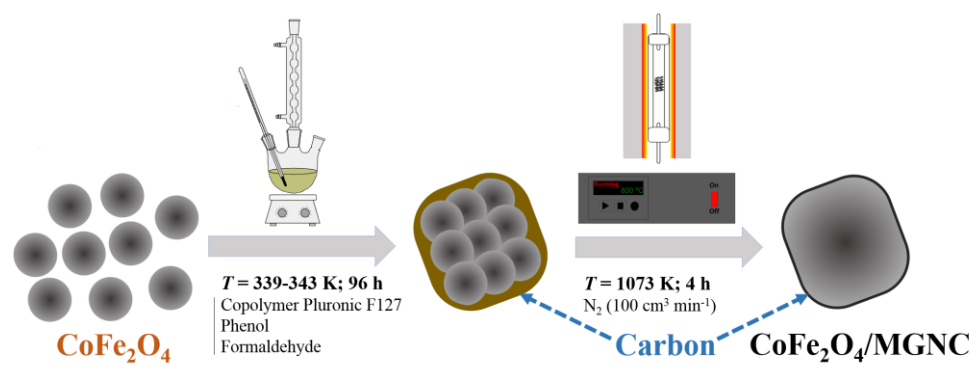
Figure 3. (a) Field- and (b) temperature-dependent magnetization curves of $CoFe_2O_4$/MGNC. The hysteresis curves given in (a) were obtained at $T = 300$ K, with $CoFe_2O_4$/MGNC before (as prepared) and after the MA-CWPO reaction stage; the zero-field-cooling (ZFC) and field-cooling (FC) magnetization curves given in (b) were obtained at $H = 100$ Oe. The inset of (a) is a zoom of the low-field region.

Figure 4. H_2O_2, 4-NP and TOC conversions obtained after 3 h in non-catalytic (non-cat), adsorption, CWPO and MA-CWPO experiments. The effect of *tert*-butanol (*t*-BuOH) on the H_2O_2 and 4-NP conversions by MA-CWPO is also shown. The room temperature during the experiments was 297.2 ± 0.4 K. The numbers in brackets refer to the solution temperature in each run. Experiments performed with $[4\text{-NP}]_0 = 5.0$ g L^{-1} and pH = 3, and, when applicable, with $[CoFe_2O_4/\text{MGNC}] = 5.0$ g L^{-1}, $[H_2O_2]_0 = 17.8$ g L^{-1} and $[t\text{-BuOH}] = 60$ g L^{-1}.

Figure 5. (a) H_2O_2, 4-NP and TOC conversions as a function of time, and evolution of (b) aromatic and (c) non-aromatic by-products of 4-NP oxidation in the MA-CWPO run performed with $CoFe_2O_4$/MGNC under the operating conditions given in Figure 4. 4-NP removals obtained in the run performed with the homogeneous solution ($[Fe^{2+}] = 1.1$ mg L^{-1} and $[Co^{2+}] = 2.1$ mg L^{-1}, corresponding to the amounts leached during the MA-CWPO run), and in the MA-CWPO run performed with bare $CoFe_2O_4$ ($[CoFe_2O_4] = 0.72$ g L^{-1}, corresponding to 14.4 wt.% of $CoFe_2O_4$/MGNC), are also given in (a) for comparison.

Figure 6. Mechanism proposed for the 4-NP removal in the (a) absence and (b) presence of an AC magnetic field. Bulk reactions between HO$^{\bullet}$ radicals and 4-NP are also represented in (a).
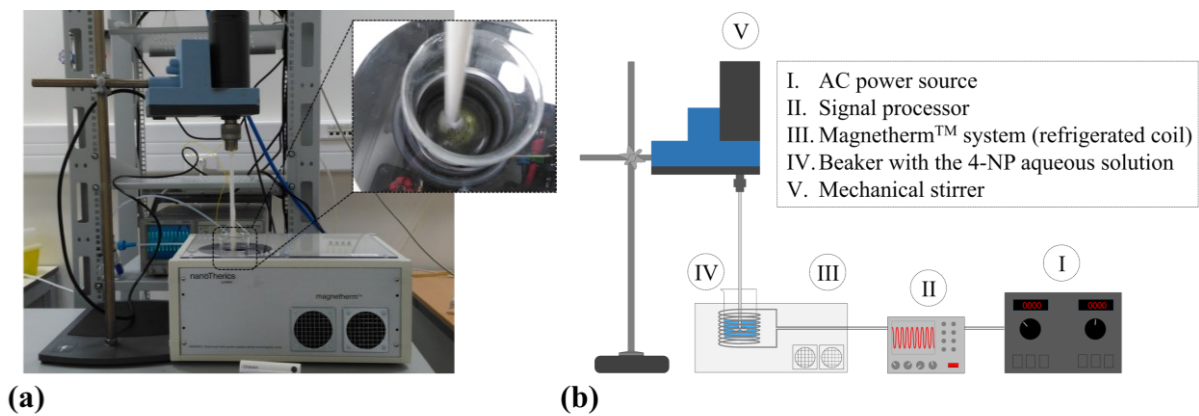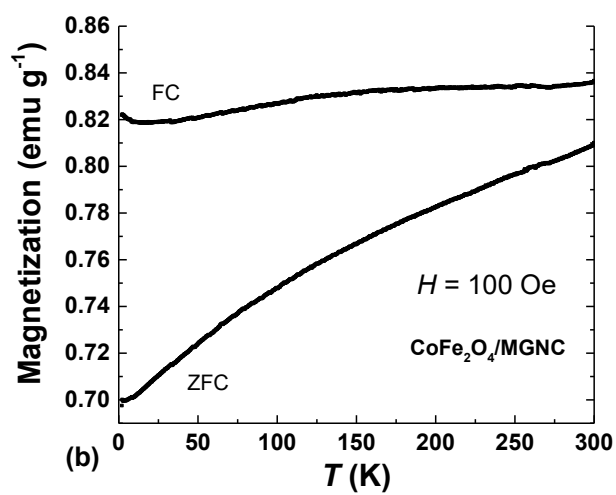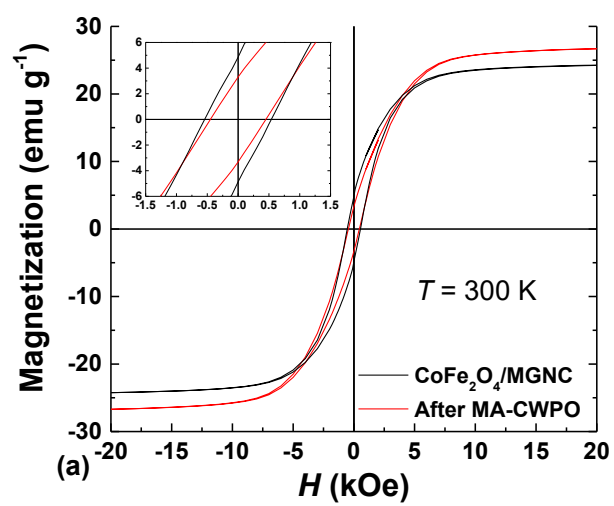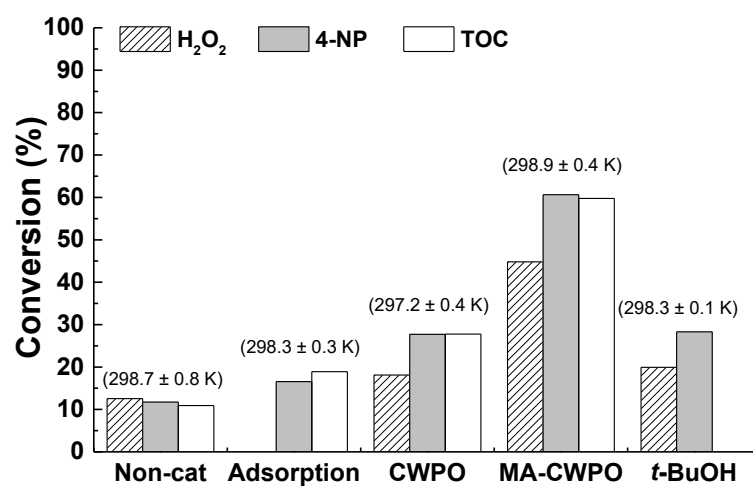
FIGURE 1

FIGURE 2

(a)   (b)

I. AC power source
II. Signal processor
III. Magnetherm™ system (refrigerated coil)
IV. Beaker with the 4-NP aqueous solution
V. Mechanical stirrer

FIGURE 3

FIGURE 4

FIGURE 5

(a)

(b)

(c)

FIGURE 6